

A Study on Fracture Behavior at the Composite Plates of CFRP and Aluminum Bonded with Sandwich Type

Teng Gao¹, Jae Woong Park², and Jae Ung Cho^{3#}

¹ Interior & Exterior, R&D Center, Hyundai Mobis China, 201615, China

² Department of Mechanical Engineering, Graduate School, Kongju National University, 1223-24, Cheonan-daero, Seobuk-gu, Cheonan-si, Chungcheongnam-do, 31080, South Korea

³ Division of Mechanical & Automotive Engineering, Kongju National University, 1223-24, Cheonan-daero, Seobuk-gu, Cheonan-si, Chungcheongnam-do, 31080, South Korea

Corresponding Author / E-mail: jucho@kongju.ac.kr, TEL: +82-41-521-9271

KEYWORDS: Carbon fiber reinforced plastic, Aluminum plate, Maximum load, Aluminum foam, Sandwich

The weight of machinery such as the aircraft, automobiles etc., has a great impact on the consumption of fuel and electricity. Thus, we have been researching on the enhanced design to make the weight of aircraft and automobile lighter. It is quite important and urgent to enhance the overall performance for the purpose of significantly reducing the weight of the machine. The aim of this study is to analyze the mechanical behavior of the aluminum plate sandwich and the carbon fiber reinforced plastic sandwich and aluminum foam specimen through the compression simulation analysis. In experiment, the maximum load of the carbon fiber reinforced plastic sandwich was 49.15 kN, the maximum load of the aluminum sandwich was approximately 51.2 kN, the maximum load of the aluminum foam specimen was 3.27 kN while the load cell moved 12 mm as the rigid displacement. It was affirmed that the results of simulation and experiment were very similar. In simulation, the maximum equivalent stress of carbon fiber reinforced plastic sandwich was larger than the equivalent stress of aluminum plate sandwich. The analysis and the experimental results obtained from this study could be applied in many areas employing CFRP and aluminum plate.

Manuscript received: March 1, 2017 / Revised: April 27, 2017 / Accepted: May 27, 2017

1. Introduction

Many studies are being conducted on composite materials with the purpose of greatly reducing the weight of a machine. Among the composite materials, there is the fiber reinforced composite material where carbon fiber, glass fiber, aramid-based fiber are used as a reinforcing material with resins such as epoxy, etc. as a matrix.¹⁻⁶ Also, a porous metallic material of aluminum foam has good characteristics such as excellent energy absorption rate, acoustic absorption and is utilized in the areas such as automobiles, vessels, aerospace, etc. This study is aimed at finding out compression characteristics for carbon fiber reinforced plastic (CFRP) composite materials having aluminum foam core and establishing the structures suitable for its application to a machine. For comparisons, the compressive characteristics for aluminum plate sandwich composite material and aluminum foam specimen were shown by producing aluminum plate sandwich composite material having aluminum foam core and Al6061-T6 employed for machinery and vessels.⁷⁻¹² Sheet material and core of the sandwich are joined by an adhesive, since the aluminum foam can be damaged if the connection method with bolts and nuts is applied to it.

Because CFRP and aluminum foam are shown to be weak at the mechanical and surface manufacturing, they must be reinforced with the homogeneous material. Therefore, connection of aluminum foam and other materials with an adhesive is more efficient.¹³⁻¹⁷ In addition, it was verified that loads and deformations were similar to the experimental data by conducting compression analysis through ANSYS with the finite element model supposing the same material properties as those of the experimental material. Here, buckling and fracture behavior occurring during compression of the material were also to be realized by the analysis.

2. Experimental Setup

Test specimens used in the present compression experiments were CFRP sandwich and aluminum plate sandwich with the structure of the sheet material being joined to both sides of the core by an adhesive as shown in Fig. 1, while there were aluminum foam specimens without the sheet material separately. Shown in Fig. 2 are the actual pictures of 3 types of specimens used in this study, where figure a is the CFRP

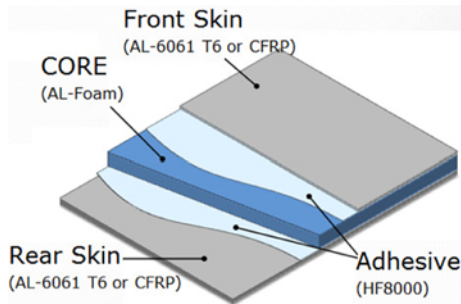


Fig. 1 Structure of sandwich specimen

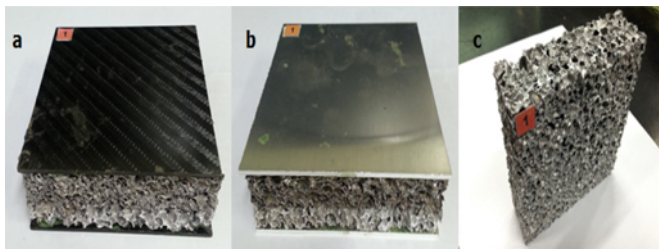


Fig. 2 Configuration of specimen

sandwich, figure b the aluminum plate sandwich, figure c the aluminum foam specimen. Because the composition of figure C is different from figure a and figure b, Figure c is not the sandwich type. Three types of test specimen were 100 mm in length and width. Also, the angular arrangement of fibers for the CFRP plate in the present study consisted of $[0/90/90/0]$. For example, the plate consisting of the $[0/90/90/0]$ method was a test specimen configured with arrangement where the first, the second, the third, the fourth layers had the respective angular orientation of 0° , 90° , 90° and 0° in that order. As the unidirectional CFRP has the strongest strength at the fiber direction, it has the stacking angle of 90° . At the stacking angle of 0° , the buckling during the manufacturing process of CFRP plate can be prevented. The adhesive used in this study is HF8000. As the injection time of adhesive is 10 seconds, the adhesive thickness becomes same at all cases.

The equipment employed for compression experiments was a universal material tester of SHIMADZU AG-X with the maximum capacity of 250 kN. The necessary material properties (mechanical properties) were obtained from the present experimental equipment by compressing until fracture occurred by the gradual application of loads to the specimen having a determined size and form. Also, the relationships between resistance force resisted by the material and deformation as well as compressive strengths, etc. could be measured through the load cell. The configuration of experimental equipment is as shown in Fig. 3. Composite material test pieces of CFRP sandwich, aluminum plate sandwich and aluminum foam specimen were placed on the flat plate as shown in Fig. 4, and compressive experiments were conducted in vertical direction while the load cell was descended at the rate of 1 mm/min. With the slow static displacement speed, the fracture behavior can be checked accurately. The enforced displacement speed is 1 mm/min. To obtain accurate data, all test specimens were made to be positioned at the axis center of the circular plate load cell, and three specimens were subjected to the experiments under the same condition

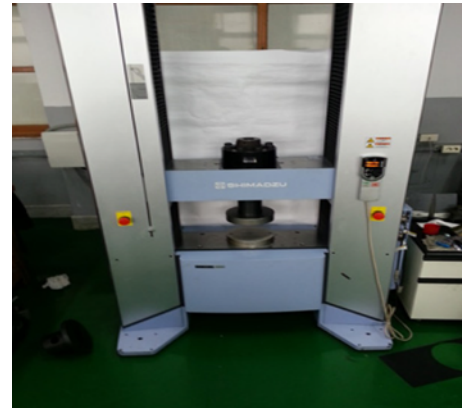


Fig. 3 Experimental apparatus

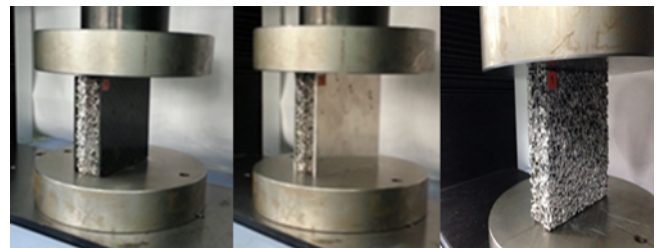


Fig. 4 Picture of installed specimens at compression experiment

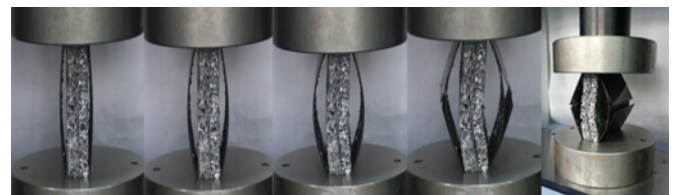


Fig. 5 Experimental pictures of carbon fiber reinforced plastic sandwich

for each experiment. At the state composed of only the jig prior to the experiment, the apparatus is compensated. As the experiment is carried out after the adjustment of zero point, the flat plate does not have the influence on the experimental apparatus.

3. Experimental Results

Fig. 5 shows an appearance of the composite material being damaged in the compression experiment process for the test piece of CFRP sandwich composite material when the load cell moved by 12 mm. While the load cell was descending, the debonding phenomenon occurred between the CFRP and the aluminum foam, and clipping of fiber layers on both sides of the specimen could be observed. It could also be seen that cell walls collapsed in the center part of the aluminum foam of the specimen, producing relative displacements.

Fig. 6 shows an appearance of the composite material being damaged in the compression experiment process for the test piece of aluminum plate sandwich composite material when the load cell moved

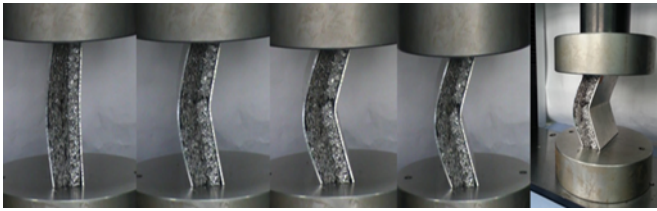


Fig. 6 Experimental pictures of aluminum plate sandwich

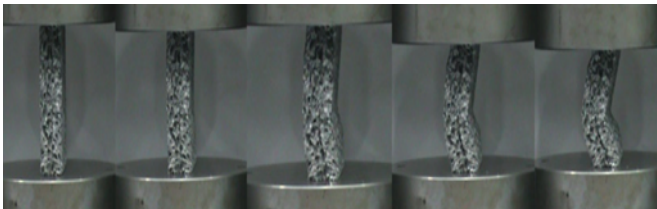


Fig. 7 Experimental pictures of aluminum foam specimen

by 12 mm. Unlike the experimental results for CFRP sandwich composite material, no debonding phenomenon occurred between the sheet material and the core in the test piece of aluminum plate sandwich composite material, and overall occurrence of buckling in the specimen was visible. The reason is that fine dust or pores are incorporated in the aluminum plate during production process of the latter. Buckling occurred during compression process in the aluminum plate which was affected by pores. The deformation direction due to the buckling of aluminum plate propagated as the same direction as deformation of aluminum foam. The falling off of bonding surface did not happen greatly like CFRP.

Fig. 7 shows an appearance of the composite material being damaged in the compression experiment process for the test piece of aluminum foam composite material when the load cell moved by 12 mm. From Fig. 7, it could be seen that cell walls collapsed in the center part of the aluminum foam producing relative displacements when there was no sheet material. Accordingly, the cells in the center part of aluminum foam are considered to be broken more easily in the compression process. Also, the aluminum foam specimens showed an overall aspect of occurrence of buckling as the load cell was descended.

Fig. 8 shows changes in compression loads while three types of specimen were displaced by 12 mm. In the compression process, the maximum load for CFRP sandwich was 49.15 kN, that for aluminum plate sandwich 51.21 kN, and that for aluminum foam specimen 3.27 kN. The maximum loads for CFRP sandwich and aluminum plate sandwich were affirmed to have occurred around the displacement of 1.5 mm. Considering the load curve for CFRP sandwich, the load can be seen to be maintained at about 10kN from the displacement of 2 mm through that of 9 mm, while it dropped drastically at the displacements of 9.18 mm and 11.35 mm. The reason is attributed to the clipping of fibers of CFRP at the displacements of 9.18 mm and 11.35 mm. The clipped shape of fibers of CFRP can be observed in Fig. 5. The difference of maximum load between CFRP sandwich and aluminum plate sandwich is 2.06 kN. This difference is the reason why the density of material became higher with the compression as CFRP had the brittleness and aluminum plate had the ductility. The fracture of CFRP

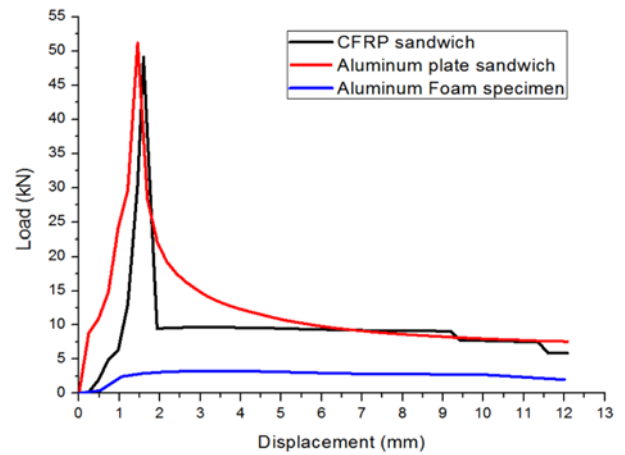


Fig. 8 Graph of load vs. displacement for experiment of carbon fiber reinforced plastic sandwich, aluminum plate sandwich, aluminum foam specimen

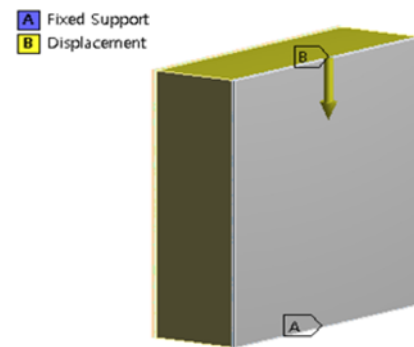


Fig. 9 Analysis condition of model

happened as it was, regardless of the material density. In other words, the maximum load on the compression of material was shown to be great immediately prior to the buckling at the aluminum plate sandwich. On the contrary, the maximum load at CFRP sandwich happened with the falling off of bonded surface. The maximum load at aluminum plate sandwich was shown to be faster and higher than CFRP sandwich.

4. Boundary Condition and Results of Simulation

4.1 Boundary condition for the simulation

Fig. 9 shows the boundary conditions for analysis. In Figs. 4-9, the bottom of CFRP sandwich was fixed while the top was applied with the forced displacements. To increase convergence, the analysis steps were divided into 12 and one step was made to be moved by 1 mm for 1 second to give a total forced displacement of 12 mm. The debonding condition was given between the CFRP and the aluminum foam. In the case of aluminum plate sandwich and aluminum foam specimen, the same boundary conditions as those of Fig. 9 were given. As the boundary condition between the homogeneous materials, these materials were bonded each other. The debonding condition was simulated like the experimental result and the influences are checked.

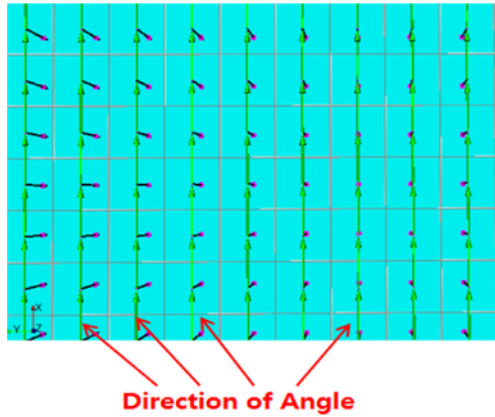


Fig. 10 Angle of carbon fiber in case of 0°

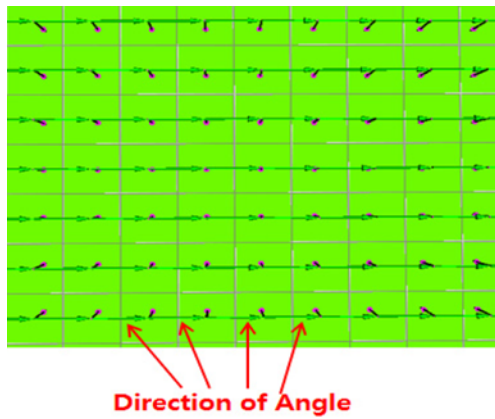


Fig. 11 Angle of carbon fiber in case of 90°

Table 1 Property of carbon fiber reinforced plastic

Poisson's ratio (v12)	0.3
Poisson's ratio (v23)	0.74
Tensile modulus (E1) (GPa)	132
Tensile modulus (E2) (GPa)	8.98
Tensile strength (Xt) (MPa)	1447
Tensile strength (Yt) (MPa)	51.72
Compressive strength (Xc) (MPa)	1447
Compressive strength (Yc) (MPa)	206.2

Table 2 Properties of aluminum foam and aluminum plate

	Al - Foam	Al - 6061 T6
Density (kg/m ³)	400	2,700
Young's modulus (MPa)	2,374	68,900
Poisson's ratio	0.29	0.33
Compressive yield strength (MPa)	1.8	276
Tensile yield strength (MPa)	1.8	276

Angular arrangement for CFRP fibers in the present study consists of [0/90/90/0], and Fig. 10, Fig. 11 are the visualized figures for 0°, 90° defined in the analysis. In Figs. 10 and 11, the arrows within the displayed layer represent the directions of fibers. Material properties of CFRP are given in Table 1, while material properties of aluminum foam and aluminum plate (Al-6061 T6) are shown in Table 2. v12 and

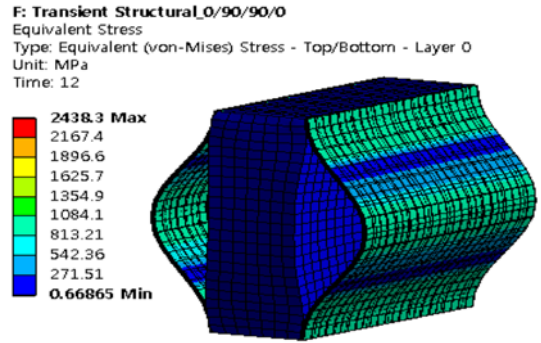


Fig. 12 Contours of equivalent stress of carbon fiber reinforced plastic sandwich

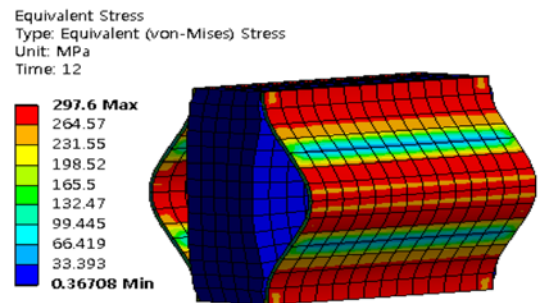


Fig. 13 Contours of equivalent stress of aluminum plate sandwich

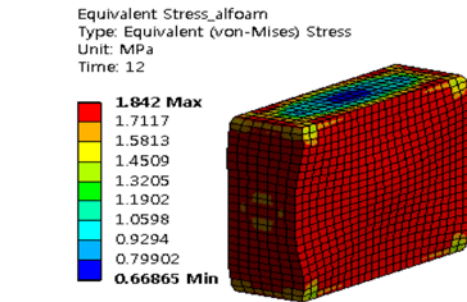


Fig. 14 Contours of equivalent stress of aluminum foam specimen

v23 shown in Table 1 are Poisson's ratios for the fiber direction and the direction perpendicular to the fiber, respectively. E1 and E2 are Young's moduli for the fiber direction and the direction perpendicular to the fiber, respectively. Xt and Yt are tensile strengths for the fiber direction and the direction perpendicular to the fiber, respectively. Xc and Yc are compressive strengths for the fiber direction and the direction perpendicular to the fiber, respectively.

4.2 Simulation results

Angular Shown in Figs. 12, 13, 14 are equivalent stress contour lines of the analysis results for CFRP sandwich, aluminum plate sandwich and aluminum foam specimen, respectively. According to Figs. 12, 13, 14, the maximum equivalent stress of 2438.3 MPa occurred in CFRP, that of 297.6 MPa in aluminum plate, and that of 1.842 MPa in aluminum foam. The maximum equivalent stress for CFRP is considered to be the largest of all. If the fracture of element happened at finite element

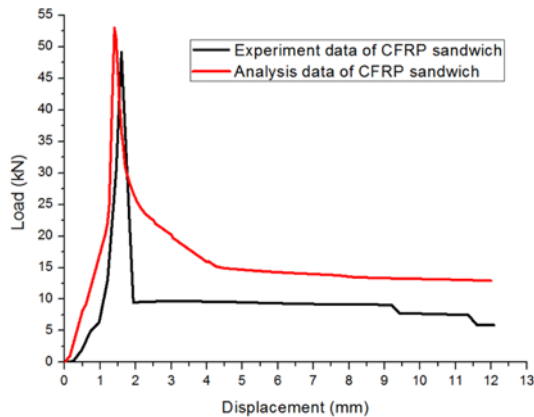


Fig. 15 Load-displacement curves of carbon fiber reinforced plastic sandwich at experimental and simulation results

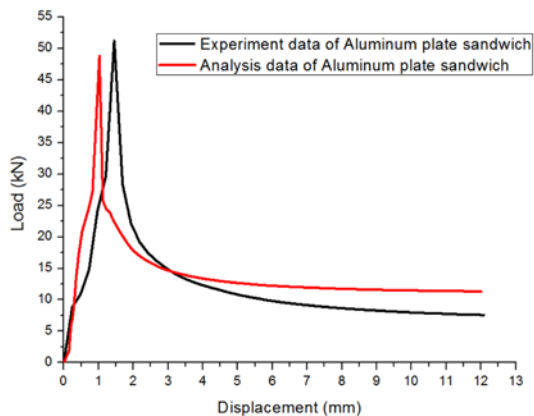


Fig. 16 Load-displacement curves of aluminum plate sandwich at experimental and simulation results

method, it was not possible to analyze. So, the fracture at the analysis of CFRP sandwich did not happen like the experiment.

Fig. 15 represents a graph for comparison of loads due to the rigid body displacement in the experiment and the analysis for CFRP. The maximum load for CFRP sandwich in the analysis was about 53 kN, while that for CFRP in the experiment was about 49.15 kN, thus affirming an error of about 7.8%. The maximum difference at the comparison of loads was shown to be about 3.51 kN. As for the reason, there were cases where pore or dust are actually incorporated in the material during the production of material, as well as external factors such as the friction forces and the characteristics of a disorder structure for aluminum foam, etc. Considering compression experiment process for the aluminum foam specimen, cell walls inside the aluminum foam were collapsed by moving as the relative displacements. In addition, since the fiber angles could not be made 100% accurately in actual production, its effects on the experiment and the analysis are thought to be great. As shown by this figure at the analysis result, the shape of graph happened like the general mild steel. This reason is the state that the finite element on analysis cannot be broken.

Fig. 16 shows a comparison of loads as a function of rigid body displacement for the experiment and the analysis of aluminum plate sandwich. The maximum load for aluminum sandwich in the analysis

was about 48.8 kN, while that for aluminum sandwich in the experiment was about 51.21 kN, thus affirming an error of 4.7%. The maximum difference at the comparison of loads was shown to be about 2.41 kN. As for the reason, buckling occurred during the experiment in the specimen due to the characteristics of a disorder structure in aluminum foam, causing the reduction in maximum load. Also, according to Figs. 15 and 16, both maximum loads in the simulation can be seen to have occurred earlier than those in the experiment. The reason is that there was a very small gap between the load cell and the test specimen in the experiments and that the specimens were not completely horizontal when prepared. And the shapes occurring in the simulation and those in the experiment of this study were affirmed to be similar. The displacement-load curve from the simulation and that from the experiment were affirmed to be similar. Consequently, the analysis results produced in this study are thought to be usable for the areas where CFRP, aluminum plate (AL 6061-T6) and aluminum foam are applied. In case of the model of aluminum plate sandwich, the buckling was configured to experiment but it was not configured to analysis. Therefore, the deviation between the analysis and experiment at the model of aluminum plate sandwich becomes higher than that of CFRP sandwich.

5. Conclusions

In this study, compression analysis was conducted for CFRP sandwich, aluminum plate sandwich, aluminum foam specimen, and the following conclusions have been derived.

According to the experimental results, the maximum load for CFRP sandwich was about 49.15 kN, that for aluminum plate sandwich about 51.21 kN, and that for aluminum foam specimen about 3.27 kN.

According to the compression simulation, the maximum load for CFRP sandwich was about 53 kN, affirming an error of 7.8% based on the experimental results. Also, the maximum load for aluminum plate sandwich in the simulation was about 48.8 kN, affirming an error of about -4.7% based on the experimental results. The reason for the larger error for CFRP sandwich is attributed to the fact that fiber angle could not be made 100% accurately in actual production which is said to have great effects on the experimental and the analysis results.

The shape occurring in the simulation of the present study was affirmed to be similar to that in experiments. Accordingly, the analysis results produced in the present study are thought to be useable for the areas where CFRP, aluminum plate (AL 6061-T6) and aluminum foam are employed. Based on combination of the analysis results, the maximum load for CFRP sandwich was shown to be greater than that for aluminum plate sandwich, and hence the structure of CFRP with the lighter weight was determined to be favorable.

ACKNOWLEDGEMENT

“This research was supported by Basic Science Research Program through the National Research Foundation of Korea (NRF) funded by the Ministry of Education, Science and Technology (2015R1D1A1A01 057607).”

REFERENCES

1. Lefanti, R., Ando, M., and Sukumaran, J., "Fatigue and Damage Analysis of Elastomeric Silent Block in Light Aircrafts," *Materials & Design*, Vol. 52, pp. 384-392, 2013.
2. Hu, H., Lu, W.-J., and Lu, Z., "Impact Crash Analyses of an Off-Road Utility Vehicle—Part II: Simulation of Frontal Pole, Pole Side, Rear Barrier and Rollover Impact Crashes," *International Journal of Crashworthiness*, Vol. 17, No. 2, pp. 163-172, 2012.
3. Han, M.-S., Choi, H.-K., Cho, J.-U., and Cho, C.-D., "Experimental Study on the Fatigue Crack Propagation Behavior of DCB Specimen with Aluminum Foam," *Int. J. Precis. Eng. Manuf.*, Vol. 14, No. 8, pp. 1395-1399, 2013.
4. Zhang, Y.-J. and Yang, C.-S., "FEM Analyses for Influences of Stress-Chemical Solution on THM Coupling in Dual-Porosity Rock Mass," *Journal of Central South University*, Vol. 19, No. 4, pp. 1138-1147, 2012.
5. Öchsner, A., Stasiek, M., Mishuris, G., and Grácio, J., "A New Evaluation Procedure for the Butt-Joint Test of Adhesive Technology: Determination of the Complete Set of Linear Elastic Constants," *International Journal of Adhesion and Adhesives*, Vol. 27, No. 8, pp. 703-711, 2007.
6. Watanabe, Y., Ichikawa, H., Kayama, O., Ono, K., Kaneoka, K., and Inami, S., "Influence of Seat Characteristics on Occupant Motion in Low-Speed Rear Impacts," *Accident Analysis & Prevention*, Vol. 32, No. 2, pp. 243-250, 2000.
7. Verver, M. M., De Lange, R., van Hoof, J., and Wismans, J. S., "Aspects of Seat Modelling for Seating Comfort Analysis," *Applied Ergonomics*, Vol. 36, No. 1, pp. 33-42, 2005.
8. Mehrabian, A., Ali, T., and Haldar, A., "Nonlinear Analysis of a Steel Frame," *Nonlinear Analysis: Theory, Methods & Applications*, Vol. 71, No. 12, pp. e616-e623, 2009.
9. Guo, L.-X., Chen, H., and Li, J.-L., "Endergonic Property Analysis of Vehicle Seat Pillow under Heads Crash Loads," *Procedia Engineering*, Vol. 15, pp. 3046-3050, 2011.
10. Hojo, M., Ando, T., Tanaka, M., Adachi, T., Ochiai, S., and Endo, Y., "Modes I and II Interlaminar Fracture Toughness and Fatigue Delamination of CF/Epoxy Laminates with Self-Same Epoxy Interleaf," *International Journal of Fatigue*, Vol. 28, No. 10, pp. 1154-1165, 2006.
11. Ohno, N., Okumura, D., and Niikawa, T., "Long-Wave Buckling of Elastic Square Honeycombs Subject to In-Plane Biaxial Compression," *International Journal of Mechanical Sciences*, Vol. 46, No. 11, pp. 1697-1713, 2004.
12. Tlustý, J., Smith, S., and Zamudia, C., "Operation Planning Based on Cutting Process Model," *Annals of the CIRP*, Vol. 39, No. 12, pp. 517-521, 1990.
13. Kim, S.-S., Han, M.-S., Cho, J.-U., and Cho, C.-D., "Study on the Fatigue Experiment of TDCB Aluminum Foam Specimen Bonded with Adhesive," *Int. J. Precis. Eng. Manuf.*, Vol. 14, No. 10, pp. 1791-1795, 2013.
14. Cho, H. S. and Cho, J. U., "The Characteristics of Shear Adhesive Interface Fracture of Aluminum Foam DCB Bonded Using a Single-Lap Method," *Int. J. Precis. Eng. Manuf.*, Vol. 15, No. 7, pp. 1345-1350, 2014.
15. Lee, J. H. and Cho, J. U., "Fracture Behavior on the Structures of DCB Jointed with Aluminum Foam in Tearing Mode," *Int. J. Precis. Eng. Manuf.*, Vol. 17, No. 7, pp. 897-902, 2016.
16. Lee, J. H. and Cho, J. U., "A Study on Mechanical Characteristics of Aluminum Foam Jointed by Adhesive Per Thickness under Compression," *Int. J. Precis. Eng. Manuf.*, Vol. 17, No. 8, pp. 995-1000, 2016.
17. Cho, J.-U., Cho, C.-D., and Han, M.-S., "Study of Dynamic Crack Propagation in 3PB Steel Specimens Loaded by Impact," *Int. J. Precis. Eng. Manuf.*, Vol. 10, No. 2, pp. 67-72, 2009.